Numerical modelling of Tb^{3+} doped selenide-chalcogenide multimode fibre based spontaneous emission sources

S. Sujecki[1,2], L. Sojka[1], E. Beres-Pawlik[1], H. Sakr[2], Z. Tang[2], E. Barney[2], D. Furniss[2], T.M. Benson[2], A.B. Seddon[2]
[1]Department of Telecommunications and Teleinformatics, Faculty of Electronics, Wroclaw University of Science and Technology, Wyb. Wyspianskiego 27, 50-370 Wroclaw, Poland
[2]George Green Institute for Electromagnetics Research, The University of Nottingham, University Park, NG7-2RD, Nottingham, UK

***Abstract*—We develop a model of a terbium (III) ion doped selenide chalcogenide glass fibre source that provides spontaneous emission within the mid-infrared (MIR) wavelength range. We use two numerical algorithms to calculate the solution and compare their properties.**

I. INTRODUCTION

There are many applications for mid-infrared (MIR) light sources in medicine, biology, environment monitoring, food security and defense. There are many types of light sources potentially available for MIR wavelength range, which include fibre lasers. A large effort has been invested into the development of MIR lanthanide doped fibre lasers. Many pumping schemes have been proposed for this purpose. So far, the success in this field of research is limited to operating wavelengths less than 4 µm. However, the spontaneous emission MIR light fibre sources recently realised using lanthanide ion doped multimode fibres have exceeded the 4 µm barrier and found applications in sensor technology [1,2]. Such sources are potentially highly reliable, low cost, and robust. In this contribution using a numerical model we study the luminescence properties of selenide-chalcogenide glass fibres doped with terbium (III) ions applied as wide spectrum spontaneous emission MIR light sources covering the wavelength range stretching from 4 µm to 5.5 µm. Such a system was shown recently to offer a very simple pumping mechanism [3].

For this purpose we fabricated selenide chalcogenide glass terbium doped multimode fibre and bulk samples and performed absorption and photoluminescence spectrum measurements. From the experimental results using Judd-Ofelt theory and McCumber and Fuchtbauer-Ladenburg theory we extracted the absorption and emission cross section spectra for the relevant transitions and the photoluminescence lifetimes. The details of this procedure are provided in [3]. Using experimentally derived set of parameters we realised a lanthanide doped multimode fibre numerical model based on the rate equations approach. Using the model we performed a numerical analysis of the MIR spontaneous emission fibre source, whereby we compared two methods of numerically calculating a solution of the set of ordinary differential equations. One of them consists in calculating the rigorous solution subject to the given boundary conditions while the other one is based upon an approximate approach presented in [4], which relies on the assumption of the low intensity of the signal flux. The results show the limitations of the approximate approach.

II. MIR FIBRE SOURCE MODELLING

In the case of a pump laser operating at approximately 3.0 µm wavelength and a low Tb^{3+} doping level a three-level rate equations model of the Tb^{3+} ion doped into the chalcogenide glass host may be used to calculate the level populations (Fig.1) [3]. Thus in steady state, we obtain a set of three algebraic equations that describe the system:

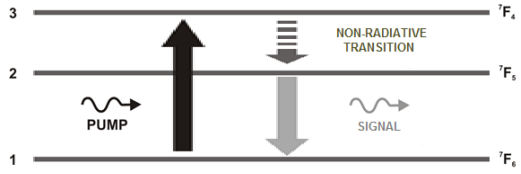

Fig. 1. Simplified energy level diagram for Tb^{3+}.

$$\begin{bmatrix} 1 & 1 & 1 \\ a_{21} & a_{22} & a_{23} \\ a_{31} & 0 & a_{33} \end{bmatrix} * \begin{bmatrix} N_1 \\ N_2 \\ N_3 \end{bmatrix} = \begin{bmatrix} N \\ 0 \\ 0 \end{bmatrix} \quad (1)$$

where N is the total dopant ion concentration while the coefficients a_{21}, a_{22}, a_{23}, a_{31} and a_{33} are obtained using the rate equations approach [3]:

$$a_{21} = \bar{\sigma}_{21a}\ \phi_s; \quad a_{22} = \bar{\sigma}_{21e}\ \phi_s - \frac{1}{\tau_{21r}} - \frac{1}{\tau_{21nr}};$$
$$a_{23} = \frac{1}{\tau_{32r}} + \frac{1}{\tau_{32nr}}; \quad a_{31} = \sigma_{31a}\ \phi_p; \quad (2)$$
$$a_{33} = \sigma_{31e}\ \phi_p - \frac{1}{\tau_{3r}} - \frac{1}{\tau_{32nr}};$$

The spatial evolution of the pump and signal photon flux are obtained from a solution of the following equations for the pump [4]:

$$\frac{d\phi_p^{\pm}}{dz} = \mp\left[\sigma_{31a}N_1 - \sigma_{31e}N_3\right]\phi_p^{\pm} \mp \alpha_p\phi_p^{\pm} \qquad (3a)$$

and the signal:

$$\frac{d\phi_s^{\pm}}{dz} = \mp\left[\overline{\sigma}_{21a}N_1 - \overline{\sigma}_{21e}N_2\right]\phi_s^{\pm} \mp \overline{\alpha}_s\phi_s^{\pm} \pm \eta N_2/\tau_2 \qquad (3b)$$

where '+' and '-' refer to forward and backward travelling waves, respectively while $\sigma_{xxa,e}$ are the relevant values of emission 'e' and absorption 'a' cross sections, α_x gives the relevant attenuation coefficient, which for the signal wave was calculated by weighing it with respect to the signal spectrum [4]. The weighting operation is marked with an overstrike symbol and was also applied consistently to the signal emission and absorption cross-section. η is the spontaneous emission coupling factor [4], τ_{xr} and τ_{xnr} are the relevant life times for radiative and non-radiative transitions, respectively. The pump and signal flux ϕ_p and ϕ_s are related to the respective power values via: $P_p = \phi_p*h*\nu_p*A$ and $P_s = \phi_s*h*\nu_s*A$ where A is the fibre cross sectional area, h – Planck's constant, ν_p and ν_s pump and signal frequency, respectively. Equations (1) and (3) are coupled and can be solved numerically subject to the relevant boundary conditions imposed at both fibre ends [5]. Alternatively, one can assume that the signal photon flux is negligibly small in (1) and hence $a_{21} = 0$ and $a_{22} = -1/\tau_{21r} - 1/\tau_{21nr}$. This assumption allows decoupling of equation (3b) from (1). Thus only equations (1) and (3a) have to be solved in a coupled way whilst equation (3b) is solved subsequently by calculating a single pass, like in the case of an amplifier, once the pump flux distribution and level populations are known [4]. This leads to a significant simplification of the numerical algorithm. However, the accuracy of such approximation has not been analysed so far. Therefore we compare both algorithms below.

The values of relevant lifetimes and cross sections were taken from [3]. The fibre was unstructured, of 200 µm outside diameter and doped with $0.95\text{x}10^{19}/\text{cm}^3$ Tb^{3+} ions, (*i.e.* circa 500 ppmw (parts per million parts by weight). The pump wavelength was 2.95 µm. The attenuation coefficient at the pump wavelength (due to the presence of the OH impurities) is 2 m^{-1}, and the weighted attenuation coefficient calculated according to [4] for the signal wave (due to SeH impurities) is 2.7 m^{-1}. The weighted signal emission and absorption cross sections are 6.3 x 10^{-25} m^2 and 6.7 x 10^{-25} m^2, respectively. The reflectivity at the fibre end for chalcogenide selenide glass is assumed to be 0.2 [5] while η =0.3 [3]. We assume that the pump light was launched at one end of the fibre whilst the MIR photoluminescence is collected at the other one.

Fig.2 shows the dependence of the calculated relative error of the approximate method: relative error = $|P_{exact}-P_{appr}|/P_{exact}$ where P_{exact} is the MIR output power calculated using the rigorous algorithm while P_{appr} is the approximate value of the output power calculated using the method presented in [4]. The length of the fibre is 2 cm. We increased the fibre end reflectivity from 0.0002 to 0.2 to study the effect of the feedback on the predicted output power and hence also the calculation error. Fig.2 shows that in accordance with the expectations the error is reduced for lower values of the fibre end reflectivity. However an error as high as 30 % can be incurred when using an approximate method for the calculation of the output power at a typical reflectivity of 0.2 for chalcogenide glass as a result of neglecting the back reflected light.

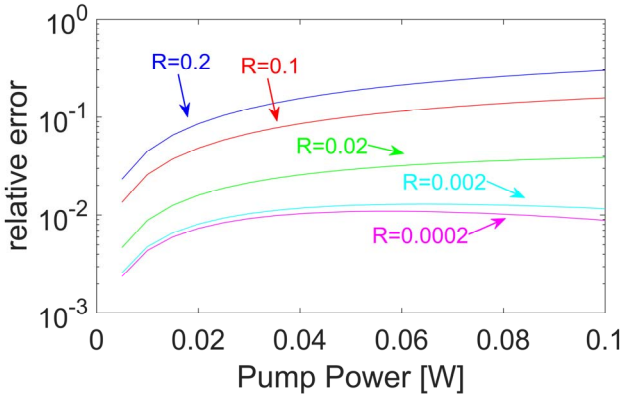

Fig. 2. The dependence of error on the pump power calculated at selected values of fibre end reflectivity R for a Tb^{3+} doped chalcogenide-selenide fibre. The fibre length is 2 cm.

ACKNOWLEDGMENT

This project has received funding from the European Union's Horizon 2020 research and innovation programme under the Marie Skłodowska-Curie grant agreement No. 665778 (National Science Centre, Poland, Polonez Fellowship 2016/21/P/ST7/03666).

REFERENCES

[1] F. Starecki, F. Charpentier, J. L. Doualan, L. Quetel, K. Michel, R. Chahal, J. Troles, B. Bureau, A. Braud, P. Camy, V. Moizan, and V. Nazabal,"Mid-IR optical sensor for CO_2 detection based on fluorescence absorbance of Dy^{3+}:$Ga_5Ge_{20}Sb_{10}S_{65}$ fibres," Sensors and Actuators B: Chemical, vol. 207, pp. 518-525, 2015.

[2] R. Chahal, F. Starecki, C. Boussard-Pledel, J. L. Doualan, K. Michel, L. Brilland, A. Braud, P. Camy, B. Bureau and V. Nazabal, "Fibre evanescent wave spectroscopy based on IR fluorescent chalcogenide fibres," Sensors and Actuators B: Chemical, vol. 229, pp. 209-216, 2016.

[3] L. Sojka, Z. Tang, D. Furniss, H. Sakr, Y. Fang, E. Beres-Pawlik, T.M Benson, A.B. Seddon and S. Sujecki, "Mid-infrared emission in Tb3+ - doped selenide glass fibre," J. of Society of America B, vol. 34, pp. 71-79, March 2017.

[4] A. L. Pele, A. Braud, J. L. Doualan, F. Starecki, V. Nazabal, R. Chahal, C. Boussard-Pledel, B. Bureau, R. Moncorge, and P. Camy, "Dy^{3+} doped GeGaSbS fibre at 4.4 µm for optical gas sensing: Comparison of simulation and experiment," Optical Materials, vol. 61, pp. 37-44, 2016.

[5] S. Sujecki, L. Sojka, E. Beres-Pawlik, Z. Tang, D. Furniss, A.B. Seddon, T.M. Benson: "Modelling of simple Dy3+ doped chalcogenide glass fibre laser for mid-inrared generation," Opt. Quant. Electron., vol. 42, pp. 69-79, January 2010.